

# Effect of cryogenic treatment on corrosion resistance of AZ61 magnesium alloy welded joint

Xiaoyuan Gong (✉ [515997393@qq.com](mailto:515997393@qq.com))

Jinzhong University

Jinming Liu

Taiyuan University of Science and Technology

Junqi Li

Foxconn (China)

Fengqing Xiao

Foxconn (China)

---

## Article

**Keywords:** welded joints, deep cryogenic treatment, microstructure, corrosion resistance

**Posted Date:** March 15th, 2022

**DOI:** <https://doi.org/10.21203/rs.3.rs-1422320/v1>

**License:** © ⓘ This work is licensed under a Creative Commons Attribution 4.0 International License.

[Read Full License](#)

---

# Abstract

The welding test of 7mm thick AZ61 magnesium alloy plate was carried out by MIG welding; the joint was cryogenically treated at  $-180^{\circ}\text{C}$ , and the holding time was 4h, 8h and 12h respectively; Weight loss method and electrochemical method were used to test the influence of cryogenic treatment on the corrosion resistance of welded joints before and after cryogenic treatment, and the corrosion morphology of specimens was observed by SEM. The test results show that the corrosion resistance of the joint sample reaches the best when the cryogenic treatment temperature is  $-180^{\circ}\text{C}$  and the holding time is 8h.

## 1. Introduction

Magnesium alloy has broad application prospect in welding equipment manufacturing and other fields. Due to the low potential of magnesium, galvanic corrosion is easy to occur. The corrosion resistance of magnesium alloy must be improved in order to expand its application[1–3].

Cryogenic treatment technology refers to the low temperature treatment method when the material is placed below  $-130^{\circ}\text{C}$ , which can stabilize the size of the material, release the residual stress and improve the toughness[4, 5]. Cryogenic treatment can change the microstructure of magnesium alloy and affect its corrosion resistance[6, 7]. The effect mechanism of cryogenic treatment on corrosion resistance of MIG welded AZ61 magnesium alloy was studied in this paper.

## 2. Materials And Processes

MB5 magnesium alloy in extruded-rolled state was used as base material, and the plate thickness is 7mm. Select a homogeneous welding wire with the base material, with a diameter of 1.6mm. MIG welding is used with CMT (Cold Metal Transfer) technology, and the welding process parameters are shown in Table 1.

Table 1  
welding parameters

	Wire feeding speed(m/min)	Current (A)	voltage (V)	Welding speed (m/min)
Backing welding	9.6	131	9.4	0.8
Cover welding	14	170	12	0.36
Swing setting	Swing length 3.5mm, swing width 4mm, jagged side swing			
Nozzle diameter	14mm			
Argon flow	14L/min			
Wire diameter	1.6mm			

In this experiment, the cryogenic treatment temperature is  $-180^{\circ}\text{C}$ , and after a period of heat preservation, it slowly rises to room temperature in the cryogenic box. The holding time is 4h, 8h and 12h respectively, and the heating rate is  $6^{\circ}\text{C}/\text{min}$ .

The corrosive medium used in the test is NaCl solution with mass fraction of 3.5%. The etching time is 24h. The corrosion rate of the sample was determined by weight loss method, and the microstructure of the sample after corrosion was observed by SEM.

The electrochemical test used a three-electrode system, the saturated meromam electrode is the reference electrode, the platinum electrode is the auxiliary electrode, and the sample is the working electrode. The sample was placed in 3.5% NaCl solution for 3min and then measured until the open circuit potential stabilized. The polarization curve is measured by potentiodynamic scanning. The scanning speed is  $10\text{mV}/\text{s}$ , and the scanning potential range is  $-2\text{V}-0\text{V}$ . As a comparison, Nyquist diagram was used to reflect the impedance spectrum of the sample to compare the corrosion resistance of the joint sample before and after cryogenic treatment in 3.5%NaCl medium.

### 3. Results And Analysis

#### 3.1 Corrosion morphology and result analysis

By Fig. 1(a) and (b), the lower part of the two figures is the weld area, and the upper part is the heat affected zone and a small amount of base metal area. the weld area has the best corrosion resistance in the three areas and poor corrosion resistance in the other two areas, corrosion steps can be seen near the joint fusion line. The corrosion degree of the joint after cryogenic treatment is less than that of the untreated joint, Moreover, the corrosion in the three areas of the joint is relatively uniform on the whole, and the corrosion steps still exist, but not obvious. It can be seen that the welded joint after cryogenic treatment has good corrosion resistance, and the threat of local corrosion fracture of the joint is reduced due to the homogenization of corrosion.

#### 3.2 corrosion weight loss test results and analysis

Table 2  
summary of corrosion rate data

	Untreated	$-100^{\circ}\text{C}$	$-140^{\circ}\text{C}$	$-180^{\circ}\text{C}$
4h	0.2545	0.1964	0.1478	0.1299
6h		0.1494	0.1291	0.0873
8h		0.1248	0.0764	0.0516

As shown in Table 2, after corrosion in 3.5% NaCl solution for 24h, the joint samples with cryogenic treatment parameter of  $-180\text{ }^{\circ}\text{C}$  for 8h have the best corrosion resistance, and the corrosion rate is about 5 times lower than that of untreated samples.

### 3.3 Electrochemical test and result analysis

From Fig. 2(a), with the extension of the deep cold treatment time, the grain is refined, the self-corrosion potential of the joint sample is constantly negative shift, the corrosion current is gradually reduced, the width of the passivation steps is gradually increasing, the maximum value is reached when the time is 8h. Under this parameter, the protective film layer on the surface of the joint is the most stable and the corrosion resistance is the best. The difficulty of the cathodic reaction affects the corrosion rate of the joint sample. As can be seen from the figure that the cathodic reaction rate of different cryogenic parameters gradually decreases with the increase of cryogenic treatment time. Similarly, as shown in Fig. 2(b), with the decrease of cryogenic treatment temperature, the self-corrosion potential and self-corrosion current generally show a decreasing trend, the cathode branch curve shows a decreasing trend, the resistance of cathode hydrogen evolution reaction increases, and the hydrogen evolution corrosion rate of cathode gradually decreases. When the parameter is  $-180\text{ }^{\circ}\text{C}$  for 8h, The corrosion resistance of the alloy is the best (the self corrosion potential is reduced by  $0.017\text{v}$  compared with the untreated joint sample, and the corrosion current density is reduced by one order of magnitude), the passivation range is the most obvious, and the logarithm of corrosion current density is the lowest.

Since charge transfer and corrosion film are formed on the surface of the sample, the equivalent circuit is used to verify, and two sets of parallel resistors and capacitors are used to form a parallel circuit, as shown in Fig. 3,  $R_s$  is the solution resistance,  $R_{ct}$  is the charge transfer resistance,  $R_{film}$  is the protective resistance formed by the corrosion film,  $C_{dl}$  is the electric double-layer capacitance, and  $C_{film}$  is the corrosion film capacitance.

$$C_{PE} = C_{film} C_{dl}$$

Table 3  
Fitting result of  $R_{ct}$  and  $R_{film}$  of the joint by deep cryogenic of 8h for different holding time

	$R_{ct}(\text{ohm cm}^2)$	$R_{film}(\text{ohm cm}^2)$
untreated	920	2089
$-100\text{ }^{\circ}\text{C}$ , 6h	1036	2103
$-140\text{ }^{\circ}\text{C}$ , 6h	1251	2175
$-180\text{ }^{\circ}\text{C}$ , 6h	1384	2631

Figure 4 shows the impedance spectrum of joint samples insulated for 6h at different cryogenic treatment temperatures, and the untreated samples are used as comparison. The diameter of the semicircular arc in the impedance spectrum is proportional to the electron transfer resistance, and the larger the diameter, the harder the sample is to be corroded[8, 9]. The diameter of the semi-circular arc was continuously increased during the cryogenic treatment, and the corrosion resistance of the sample gradually became better. When the cryogenic parameter is  $-180^{\circ}\text{C}$  for 6h, the semi-circular arc diameter is the largest and its corrosion resistance is the best. Table 3 shows the fitting results of the impedance values before and after cryogenic treatment by the corrosion current density calculation formula. Taking the untreated sample as a reference, when the cryogenic treatment parameter is  $-180^{\circ}\text{C}$  for 6h, the corresponding  $R_{ct}$  and  $R_{film}$  are the maximum.

Table 4  
Fitting result of  $R_{ct}$  and  $R_{film}$  of the joint by deep cryogenic at  $140^{\circ}\text{C}$  for Different Time

	$R_{ct}(\text{ohm cm}^2)$	$R_{film}(\text{ohm cm}^2)$
untreated	920	2089
$-140^{\circ}\text{C}$ , 4h	1093	2041
$-140^{\circ}\text{C}$ , 6h	1251	2175
$-140^{\circ}\text{C}$ , 8h	1591	3382

Figure 5 shows the impedance spectrum of joint samples insulated for different times at  $-140^{\circ}\text{C}$ , with the extension of cryogenic treatment time, the diameter of semicircular arc increases and the corrosion resistance of the sample improves. The best corrosion resistance is  $-140^{\circ}\text{C}$  for 8h. According to the calculation formula of corrosion current density, the impedance values before and after cryogenic treatment were fitted, as shown in Table 4. With the extension of cryocooling treatment time, both  $R_{ct}$  and  $R_{film}$  increased, and the corrosion resistance of the joint gradually became better. The distribution of  $\beta$ -phase and grain size affect the corrosion resistance of the sample. When the continuous distribution of  $\beta$ -phase is relatively rare and the grain size is large, it is difficult to block the corrosion of the  $\alpha$  phase in the  $\text{Cl}^-$  environment, Cryogenic treatment improves the microstructure of the joint and the distribution of  $\beta$ -phase, making the  $\beta$ -phase finely dispersed and strengthening the corrosion barrier effect of  $\beta$ -phase relative to  $\alpha$ -phase. Cryogenic treatment also makes the structure uniform and refined, and improves corrosion resistance.

## 4 Conclusions

(1) The morphology and distribution of  $\beta$ -phase are changed during the welding process. The  $\beta$ -phase in the weld zone showed a continuous network distribution morphology, and the corrosion resistance was improved, while the  $\beta$ -phase in the HAZ zone showed a block-shaped discontinuous distribution morphology, and the corrosion resistance was decreased. In addition, when the content of  $\beta$ -phase is small, the microgalvanic corrosion effect between the two phases is obvious, but with the content of  $\beta$ -phase increases, the effect of blocking spot corrosion is also enhanced, which can be used as a corrosion barrier to prevent the depth of corrosion developing.

(2) The joint structure is obviously refined after cryogenic treatment, and, the refining effect becomes more obvious with lower temperature and longer treatment time. The refined joint structure can effectively inhibit the cathodic hydrogen evolution reaction in electrochemical corrosion, and improve the corrosion resistance of the joint by increasing the reaction resistance.

(3) When the cryogenic treatment parameter is  $-180^{\circ}\text{C}$  for 8h, the corrosion rate of the joint decreases by about 5 times compared with the untreated sample, the corrosion potential increases by about 0.11V compared with the untreated sample, and the corrosion current density decreases by 1 order of magnitude from  $6.798 \cdot 10^{-6} \text{A} \cdot \text{cm}^{-2}$  to  $5.602 \cdot 10^{-7} \text{A} \cdot \text{cm}^{-2}$ .

## Declarations

## Acknowledgements

The authors acknowledge the financial support from Scientific and technological innovation projects of colleges and universities in Shanxi Province (No. 2020L0610), and The Collaborative Innovation Center for the modified application of lightweight materials.

## Data Availability

all data reported in this study are available upon request by contact with the corresponding author.

## Author Contributions:

Xiaoyuan Gong conceived and designed the experiments; Xiaoyuan Gong and Jingming Liu performed the experiments and analyzed the data; Junqi Li and Fengqing Xiao contributed materials and analysis tools; Xiaoyuan Gong wrote the paper.

## Conflicts of Interest:

All four authors claim that there is no conflict of interest.

## References

1. Kish, J. R. , Williams, G. , Mcdermid, J. R. , Thuss, J. M. , & Glover, C. F. . (2014). Effect of grain size on the corrosion resistance of friction stir welded mg alloy az31b joints. *Journal of the Electrochemical Society*, 161(9), C405-C411. <https://doi.org/10.1149/2.0901409jes/meta>
2. Liu, J. , Hu, H. , Liu, Y. , Zhang, D. , & Zhi, Y. . (2020). Mechanical properties and wear-corrosion resistance of a new compound extrusion process for magnesium alloy az61. *Materials Testing*, 62(4), 395-399. <https://doi.org/10.3139/120.111476>
3. Dhanapal, A. , Rajendra, B. S. , Balasubramanian, V. , Chidambaram, K. , & Thoheer, Z. . (2013). Experimental investigation of the corrosion behavior of friction stir welded az61a magnesium alloy welds under salt spray corrosion test and galvanic corrosion test using response surface methodology. *International Journal of Metals*, 2013,(2013-8-24), 2013, 1-17. <https://doi.org/10.1155/2013/317143>
4. Zhang, Q. H. , Luo, L. , Liu, Y. , & Xu, Z. H. . (2021). Effect of cryogenic treatment on the microstructure and mechanical properties of extruded mg-3.5zn-0.6gd alloy. *Materials Science Forum*, 1035, 175-181. <https://doi.org/10.4028/www.scientific.net/MSF.1035.175>
5. Barylski, A. , Dercz, G. , & Kupka, M. . (2021). The sclerometrical, mechanical, and wear behavior of mg-y-nd magnesium alloy after deep cryogenic treatment combined with heat treatment. *Materials*, 14(5), 1218. <https://doi.org/10.3390/ma14051218>
6. Zhang, X. , Cano, Z. P. , Wilson, B. , Mcdermid, J. R. , & Kish, J. R. . (2017). Effect of surface preparation on the corrosion resistance of friction stir linear lap welded az31b-h24. *Canadian Metallurgical Quarterly*, 1-14. <https://doi.org/10.1080/00084433.2017.1327500>
7. De Oliveira L A , Páez, Alejandro A.Z, Antunes R A . Effect of Fluoride Conversion Treatment Time on the Corrosion Resistance of the AZ31B Magnesium Alloy[J]. *Innovations in Corrosion & Materials Science*, 2018. <https://doi.org/10.2174/2352094908666180507114212>
8. Serizawa, A. , Iwase, Y. , Sudare, T. , Saito, N. , Kamiyama, N. , & Ishizaki, T. . (2016). Effect of microstructure on corrosion resistance and heat resistance of flame-resistant ca-added magnesium alloy az61. *Journal of Japan Institute of Light Metals*, 66(1), 9-14. <https://doi.org/10.2464/jilm.66.9>
9. Barylski, A. , Dercz, G. , & Kupka, M. . (2021). The sclerometrical, mechanical, and wear behavior of mg-y-nd magnesium alloy after deep cryogenic treatment combined with heat treatment. *Materials*, 14(5), 1218. <https://doi.org/10.3390/ma14051218>

## Figures

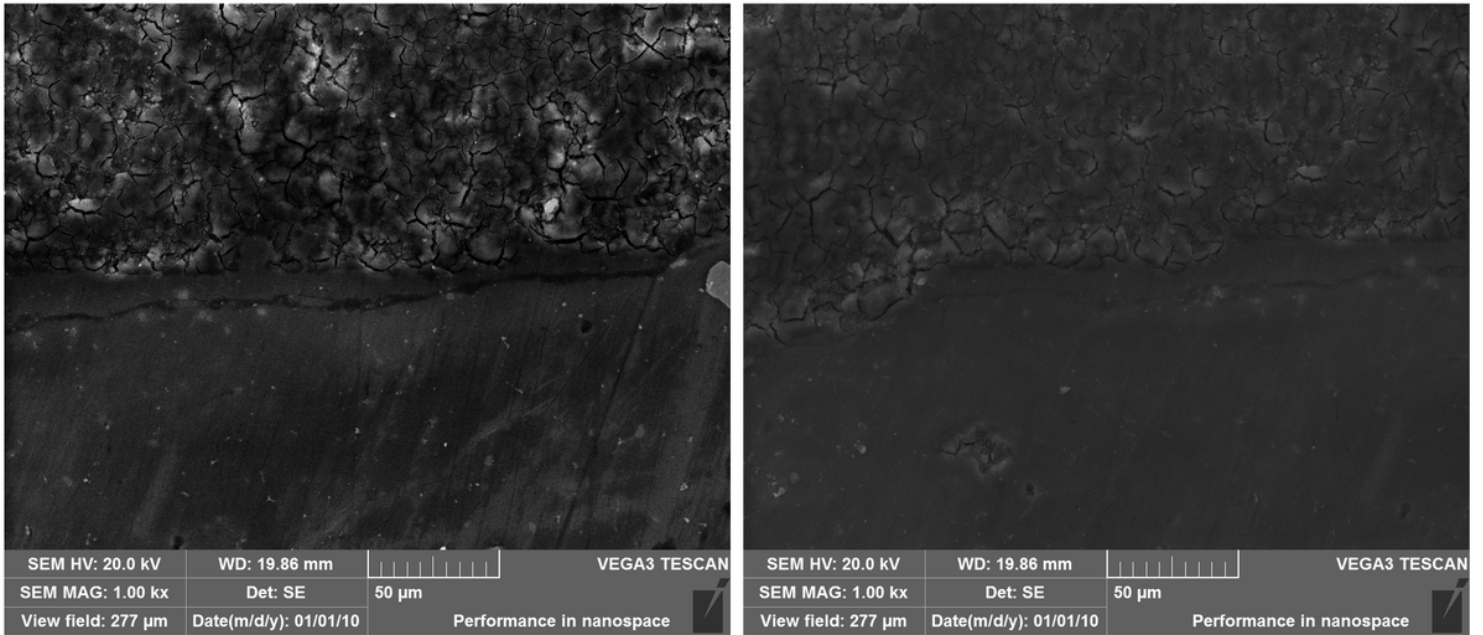


Figure 1

Figure 1 Micromorphology of the joints before and after cryogenic treatment after corrosion for 2h in 3.5% NaCl solution

(a) Before cryogenic treatment (b) After cryogenic treatment

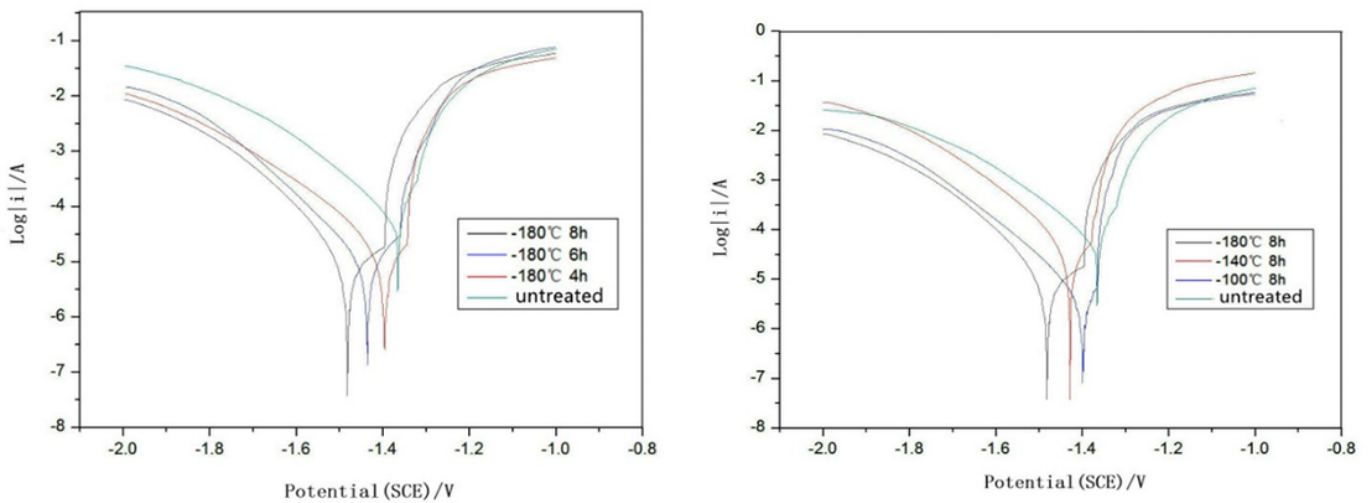


Figure 2

Impact on the polarization curve of the samples under different parameters cryogenic treatment

(a)Cryogenic treatment at different time(b)Cryogenic treatment at different temperatures

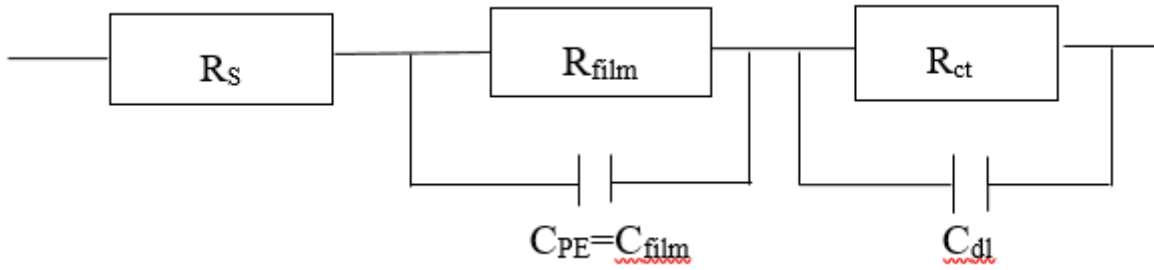


Figure 3

Equivalent circuit diagram

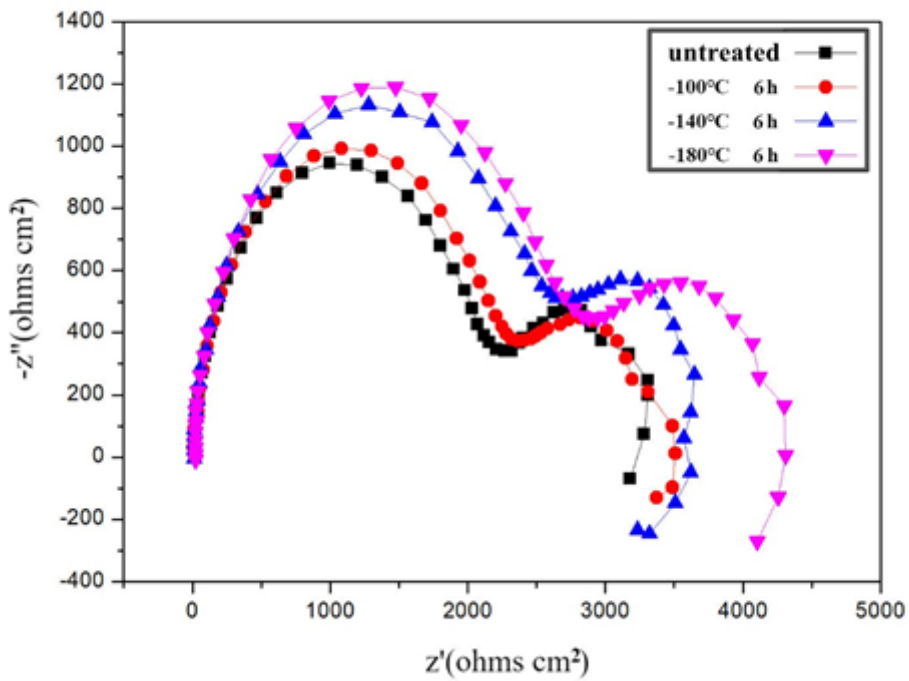


Figure 4

Impedance spectrum of the joint by deep cryogenic of 6h for different holding time

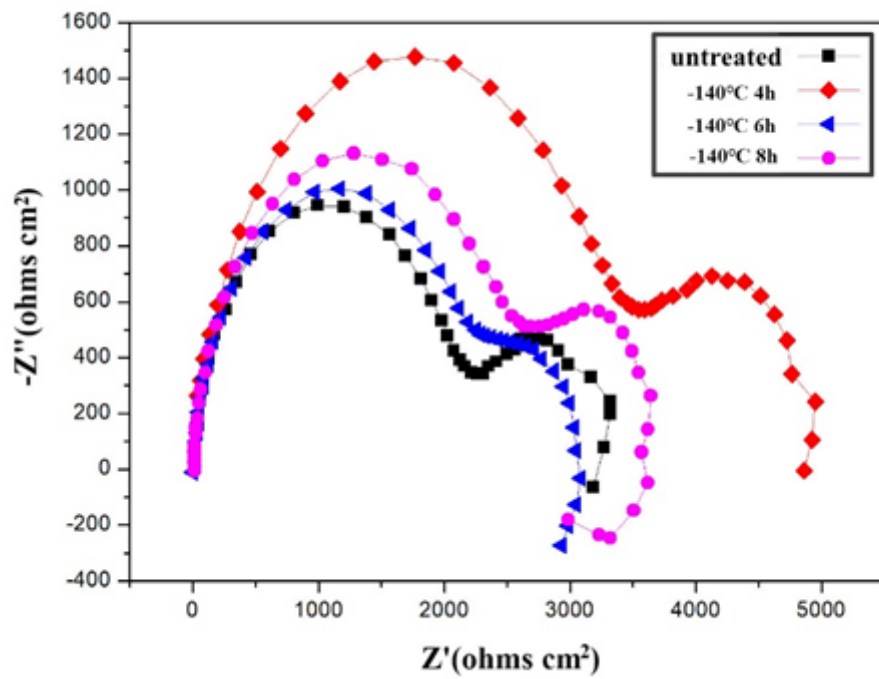


Figure 5

Impedance spectrum of the joint by deep cryogenic at 140°C for different holding time